White Rose Research Online

eprints@whiterose.ac.uk
https://eprints.whiterose.ac.uk
Universities of Leeds, Sheffield and York

Deposited via The University of Leeds.

White Rose Research Online URL for this paper:
https://eprints.whiterose.ac.uk/id/eprint/170297/

Version: Accepted Version

Article:
Yang, D, Klebl, DP, Zeng, S et al. (2020) Interplays between copper and Mycobacterium tuberculosis GroEL1. Metallomics, 12 (8). pp. 1267-1277. ISSN: 1756-5901

https://doi.org/10.1039/d0mt00101e

© The Royal Society of Chemistry 2020. This is an author produced version of a journal article published in Metallomics. Uploaded in accordance with the publisher's self-archiving policy.

Reuse
Items deposited in White Rose Research Online are protected by copyright, with all rights reserved unless indicated otherwise. They may be downloaded and/or printed for private study, or other acts as permitted by national copyright laws. The publisher or other rights holders may allow further reproduction and re-use of the full text version. This is indicated by the licence information on the White Rose Research Online record for the item.

Takedown
If you consider content in White Rose Research Online to be in breach of UK law, please notify us by emailing eprints@whiterose.ac.uk including the URL of the record and the reason for the withdrawal request.

Interplays between copper and *Mycobacterium tuberculosis* GroEL1

Dong Yang [1], David P. Klebl [2, 3], Sheng Zeng [1], Frank Sobott [2, 4, 5], Martine Prévost [6], Patrice Soumillion [7], Guy Vandenbussche [6 #] and Véronique Fontaine [1, #,*]

[1] Microbiology, Bioorganic and Macromolecular Chemistry Unit, Faculty of Pharmacy, Université Libre de Bruxelles (ULB), Brussels, Belgium

[2] The Astbury Centre for Structural Molecular Biology, University of Leeds, Leeds, UK

[3] School of Biomedical Sciences, University of Leeds, Leeds LS2 9JT, UK

[4] School of Molecular and Cellular Biology, University of Leeds, Leeds LS2 9JT, UK

[5] BAMS Research Group, Department of Chemistry, University of Antwerp, Antwerp, 2020, Belgium

[6] Laboratory for the Structure and Function of Biological Membranes, Faculty of Sciences, Université Libre de Bruxelles (ULB), Brussels, Belgium

[7] Biochemistry and Genetics of Microorganisms, Louvain Institute of Biomolecular Science and Technology, Université Catholique de Louvain (UCL), Louvain-la-Neuve, Belgium

[#] Equally contributed

* Corresponding author, email: vfontain@ulb.ac.be, postal address: Microbiology, Bioorganic and Macromolecular Chemistry Unit, Faculty of Pharmacy, Université Libre de Bruxelles (ULB), Boulevard du Triomphe, CP205/2, 1050 Brussels, Belgium

Table of contents entry

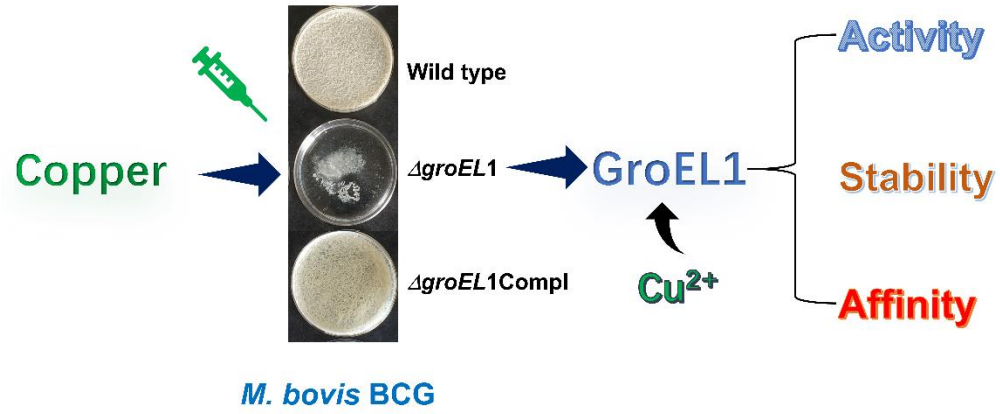

The chaperone GroEL1 enhances copper tolerance during *Mycobacterium bovis* BCG biofilm formation. The binding of copper ions to the GroEL1 histidine-rich region protects the chaperone from destabilization and increases its ATPase activity.

Abstract

The recalcitrance of pathogenic *Mycobacterium tuberculosis*, the agent of tuberculosis, to eradication is due to various factors allowing bacteria to escape from stress situations. The mycobacterial chaperone GroEL1, overproduced after macrophage entry and under oxidative stress, could be one of these key players. We previously reported that GroEL1 is necessary for the biosynthesis of phthiocerol dimycocerosate, a virulence-associated lipid and for reducing antibiotic susceptibility. In the present study, we showed that GroEL1, bearing a unique C-terminal histidine-rich region, is required for copper tolerance during *Mycobacterium bovis* BCG biofilm growth. Mass spectrometry analysis demonstrated that GroEL1 displays high affinity for copper ions, especially at its C-terminal histidine-rich region. Furthermore, the binding of copper protects GroEL1 from destabilization and increases GroEL1 ATPase activity. Altogether, these findings suggest that GroEL1 could counteract copper toxicity, notably in the macrophage phagosome, and further emphasizes that *M. tuberculosis* GroEL1 could be an interesting antitubercular target.

Introduction

Mycobacterium tuberculosis (*M. tuberculosis*) is the causative agent of tuberculosis (TB), a leading infectious disease still causing an estimated 10 million TB cases and 1.4 million deaths in 2018 [1]. This bacterial infection is difficult to treat for various reasons. First, the bacterium has an unusual impermeable cell wall that reduces drug accessibility. The mycobacterial cell wall is composed, from the inside to the outside, of peptidoglycan covalently bound to arabinogalactan which in turn can also be covalently bound to exceptionally long chain fatty acids, mycolic acids. Those are further embedded in an outer membrane, rich in non-covalently bound long fatty acids [2, 3]. Among the non-covalently embedded lipids, phthiocerol dimycocerosates (PDIM), methyl-branched fatty acid-containing lipids, are essential to resist to hostile environment and antibiotics [3-6].

In addition, this pathogen can adopt different strategies to escape bactericidal stress, *e.g.* oxidative stress within macrophages and hypoxia in lung granuloma, among others by entering into a nonreplicating state called dormancy [7-10]. The mycobacterial GroEL1 chaperonin has been previously shown to be essential for metabolic and energetic adaptation under stress, as reflected *in vitro* in a biofilm growth model [11].

M. bovis BCG and *M. tuberculosis* have two *GroEL* encoding genes, *groEL*1 (*Rv3417c*, BCG_*3487c*) in an operonic arrangement with *groES* (*Rv3418c*, BCG_*3488c*) and *groEL2* (*Rv0440*, BCG_*0479*) [12]. They encode two forms of chaperone proteins, GroEL1 (Cpn60.1, Hsp60.1) and GroEL2 (Cpn60.2, Hsp60.2), which are identical between *M. tuberculosis* and *M. bovis*. GroEL1 shares 62 % sequence identity with GroEL2 [12] and 53 % sequence identity and 70% similarity with the well-known *E. coli* GroEL[13]. The *E. coli* GroEL can oligomerize in two heptameric structures stacked back-to-back to promote protein folding with the help of the cochaperonin GroES, in an ATP-dependent manner [14-18]. The divalent cation Mg^{2+} and to a less extent Mn^{2+}, Co^{2+} or Ni^{2+}, has been shown to be required for the *E. coli* GroEL ATPase activity [19]. Interestingly, *M. tuberculosis* GroEL1 has a distinctive histidine-rich C-terminal region, while GroEL2 has a glycine-methionine-rich C-terminal region that is more typical of the GroEL chaperones [12]. In *M. tuberculosis*, both

GroEL proteins are overproduced under stress conditions, including heat shock [20], oxidative stress response [21, 22], osmotic stress [23] and during macrophage infection [24]. The *M. bovis* BCG *groEL*1 knockout mutant shows increased sensitivity to oxidative stress and vancomycin compared to the wild type strain [5]. Furthermore, our previous research demonstrated that the GroEL1 chaperone protein is required for PDIM biosynthesis as the *M. bovis* BCG Δ*groEL1* mutant is devoid of PDIM [5].

Usually, under stress, bacteria use a common virulence and adaptive factor to survive, they form biofilms [13, 22, 25, 26]. Although mycobacterial biofilms were not yet observed in patients with tuberculosis, pathologies involving nontuberculous mycobacteria were shown to be associated with biofilm infections. For pathogenic mycobacteria, biofilm has been shown to be an interesting *in vitro* growth model as, in biofilm, mycobacteria are entering into dormancy and develop adaptative bactericidal escape mechanisms like in *in vivo* stress conditions [27]. For mycobacterial biofilm formation, a high concentration of glycerol (6 % of culture medium) is used and GroEL1 was shown to be required to adapt to this high glycerol concentration [11]. In *in vivo* stress conditions, such as in the macrophage phagosome, the bacilli may encounter additional stress resulting from increased metal ion concentrations [28-30]. Although copper is essential for mycobacteria viability, the high copper ion concentration in host/cell compartments is an efficient antibacterial defence mechanism, especially against the susceptible *M. tuberculosis* [31-33].

The C-terminal histidine-rich region of GroEL1 has been predicted to be involved in metal binding [12]. This was confirmed in the purification process of *M. smegmatis* GroEL1 using Ni-agarose affinity matrix and more recently by isothermal titration calorimetry (ITC) [13, 34]. Given the overproduction of GroEL1 under stresses, we evaluated *M. bovis* BCG biofilm growth in the presence of metal ions and further investigated the impact of metal ions on GroEL1 biochemical characteristics.

Experimental section

Bacterial strains and growth condition

Wild type (wt) *M. bovis* BCG, BCG Δ*groEL*1 (KO) and BCG complemented (compl) strains were described previously [22]. *M. bovis* BCG was cultured in Middlebrook 7H9 medium (Difco Laboratories) containing 0.05% Tween 80 supplemented with 10% albumin-dextrose complex. The Δ*groEL*1 strain was grown in a medium with 25 μg/mL kanamycin, and the complemented strain with 25 μg/mL kanamycin and 50 μg/mL hygromycin.

M. bovis BCG biofilm formation

The biofilm cultures were grown on modified Sauton's medium containing 3.5% (v/v) glycerol in the presence or absence of Cu^{2+}, Zn^{2+} or Cd^{2+}. One litre of Sauton's medium contains 0.5 g KH_2PO_4, 0.5 g $MgSO_4$, 2.0 g citric acid, 0.05 g ferric ammonium citrate, 35 mL glycerol, 4.0 g asparagine, 1.435 mg $ZnSO_4$. The pH of the medium was adjusted to pH 7.2 with 1 M NaOH.

To grow biofilms in either 24-well plates or 6 cm diameter polystyrene Petri dishs, 20 μL or 100 μL of precultures (OD_{600} at 0.9-1.0) were inoculated in 2 mL or 10 mL biofilm medium. The dishes or plates were then covered twice with Parafilm® and incubated at 37 ˚C for 21-28 days without disturbance [27].

Plasmid constructions

The pET-15b vector (Novagen) was modified with a cleavage site for Rhinovirus protease 3C introduced between *NdeI* and *NcoI* in place of the thrombin cleavage site, leaving a sequence encoding a 5×His-tag [35].

The coding sequences corresponding to the *M. tuberculosis* H37Rv *groEL*1*, groEL2 and groES* genes were amplified by polymerase chain reaction (PCR). The primers used are shown in supplementary data (**Table S1**). The plasmids *p*MtGroEL1 and *p*MtGroEL1ΔHis were obtained by cloning the PCR products into the modified pET-15b vector, using the restriction sites *Nde*I and *Xho*I. The designed *p*MtGroEL1ΔHis is devoid of the last 30 bases, including the stop codon and 27 bases encoding the last 9 C-terminal amino acid residues, compared with *p*MtGroEL1. Prior to cloning, the modified pET-15b vector was linearized using the restriction enzymes *NdeI* and *BamHI*. The *M. tuberculosis groEL2* gene was cloned into the modified pET-15b vector using the In-Fusion® HD Cloning Kit (Clontech). The *M. tuberculosis groES* gene was

cloned into the modified pET-15b vector dephosphorylated by antarctic phosphatase (Anp), using the *NdeI* restriction site. The plasmids were named *p*MtGroEL2 and *p*MtGroES, respectively. All the plasmid constructions were verified by sequencing.

Protein production and purification

The constructed plasmids were transformed into *E. coli* strain BL21(DE3) for protein production. The bacteria were grown in LB medium containing 100 μg/mL ampicillin at 37 °C. Gene expression was induced with 1 mM IPTG when the optical density reached 0.5 at 600 nm. Then, the incubation was continued for 20 hours at 18 ˚C (or 30 ˚C for GroEL2). The cells were then harvested by centrifugation at 5,000 × g and resuspended in 20 mL of 20 mM HEPES, 300 mM NaCl, 20 mM $MgSO_4$, 10 mM imidazole, pH 8.0, EDTA-free protease inhibitor cocktail (Carl Roth) and 10 μg/mL DNase (Sigma).

Protein purification was always performed at 4 ˚C [36]. The resuspended cells were homogenized in a Potter-Elvehjem homogenizer and lysed by four passages through an Emulsiflex-C3 (Avestin). The lysate was collected by centrifugation at 10,000 g and loaded onto a previously equilibrated Poly-Prep column (Bio-Rad) containing 2 mL of Ni-NTA resin (Thermo Scientific). The suspension was incubated for 1 h under gentle agitation. After collecting the column flow-through, the resin was washed with 10 mM and 40 mM imidazole, in 20 mM HEPES (pH 8.0), 300 mM NaCl. The proteins were eluted with 250 mM imidazole, 20 mM HEPES (pH 8.0), 300 mM NaCl. Prior to 5 × His-tag cleavage, the buffer was exchanged for 20 mM HEPES, 150 mM NaCl (pH 7.5) on a PD-10 desalting column (GE Healthcare). Then the protein was incubated overnight at 4 ˚C with protease 3C (protein/enzyme mass ratio of 75:1) for His-tag removal. The protein was further purified on size exclusion chromatography (SEC) using a Superdex 200 10/300 GL analytical column connected to an ÄKTA purifier system (GE Healthcare). The protein solution was eluted with a selected buffer or solution (A: 50 mM Tris-HCl, 150 mM NaCl, pH 7.5 or B: 10 mM ammonium acetate, pH 6.9).

The purified proteins were flash-frozen in liquid nitrogen and stored at -80 ˚C. Protein concentrations were determined using the calculated extinction coefficients [37] at 280 nm: 16,960 $M^{-1}cm^{-1}$ for GroEL1 and GroEL1ΔHis, 11,460

$M^{-1}cm^{-1}$ for GroES and 15,930 $M^{-1}cm^{-1}$ for GroEL2. The purity and the integrity of recombinant proteins were determined by SDS-PAGE and denaturing mass spectrometry, respectively.

Mass spectrometry

Borosilicate nano-electrospray capillaries (Thermo Scientific) were prepared in-house using a P-97 micropipette puller (Sutter Instrument Co.) and coated with gold/palladium in a Polaron SC7620 sputter coater (Quorum Technologies). Mass spectrometers were operated in positive ion mode.

For intact mass determination, proteins were solubilized in a 50 % acetonitrile/1% formic acid (v/v) mixture after being desalted on ZipTipC4 (Millipore). Mass spectra were acquired on a Q-TOF Ultima mass spectrometer, typically using a capillary voltage of 1.8-2.0 kV and cone voltage of 50 V. The TOF analyzer was operated in the V mode. Molecular masses were determined after MaxEnt1 deconvolution of the raw m/z data (Waters).

For initial metal ion-binding studies, the protein was buffer exchanged into 10 mM ammonium acetate pH 6.9 via size exclusion chromatography. Native mass spectra were acquired on a Q-TOF Ultima mass spectrometer (Waters) using the settings described above. The metal binding specificity of proteins was determined, and each protein and metal ion were mixed at a final concentration of 10 μM. Metal ion solutions were prepared using $CoCl_2$, $ZnCl_2$, $NiCl_2$ and $CuCl_2$ salts.

Copper-binding was studied more in depth using an Orbitrap Q Exactive Plus UHMR modified for high mass range (Thermo Scientific). The protein was buffer-exchanged via SEC as described above or using two consecutive Zeba spin desalting columns (Thermo Scientific) and used at a final concentration of 7.5 μM in 500 mM ammonium acetate pH 6.9. This was found to produce less unfolded protein and allowed copper binding. Typical instrument settings were - 1.7 kV capillary voltage, - 50 V in source trapping, HCD was off and the AGC target set to 106 with a maximum inject time of 500 ms. The mass range was 2000 – 20000 m/z to allow detection of high oligomeric species if present. Raw data were analysed and processed using UniDec [38]. $CuCl_2$ was added to the sample to make final concentrations between 1.9 and 30 μM. Similar conditions were used to study the binding of Cd^{2+} to GroEL1.

The effect of copper ion on protein thermal stability

The thermal shift assay in the presence of the fluorescent SYPRO orange dye (Invitrogen) was used to monitor protein stability [39]. The assay was conducted in 96-well plates using the CFX96TM real-time PCR system (Bio-Rad). Briefly, 25 μL of reaction mixture contained 5 μM protein (GroEL1 or GroEL1ΔHis), 0.3 μL of 5000 × SYPRO Orange, with 10 μM Cu^{2+} in 5 mM HEPES, pH 7.5. The thermocycle parameters were set up as follows: 20 minutes pause at 10 ˚C, followed by a melt curve recorded from 10 ˚C to 95 ˚C, with 1 ˚C increase every minute, then pause at 10 ˚C for 10 minutes. The fluorescence intensity was recorded at Ex/Em = 465/510 nm. The data were obtained from the Bio-Rad Precision Melt Analysis software 1.0 and exported as Microsoft Excel spreadsheet.

Trypsin digestion susceptibility assay

To investigate the effect of copper ions on protease digestion susceptibility, a trypsin digestion assay was performed as previously described with minor modifications [40] on GroEL1 or GroEL1ΔHis in the presence or absence of Cu^{2+} at 37 ˚C. Briefly, the reaction mixture contained 5 μg GroEL1 or GroEL1ΔHis, 0.0015 μg trypsin (a mass ration of protein to trypsin was 10,000:3), in the presence or absence of $CuCl_2$. The reaction was terminated at various times by adding 1.5 μL of 50 mM PMSF and 7.5 μL SDS-PAGE Laemmli buffer (2×) to 6 μL aliquots of the reaction mixture, and the resulting solution was immediately frozen in liquid nitrogen. The samples were finally analysed by SDS-PAGE on a 15 % polyacrylamide gel. In addition, the influence of copper on trypsin activity was evaluated using *Nα*-benzoyl-DL-arginine 4-nitroanilide hydrochloride (BAPNA, Sigma) as substrate [41].

ATPase activity assay

The ATPase activities of the purified recombinant mycobacteria GroEL (GroEL1, GroEL1ΔHis, GroEL2) were quantified using a slightly modified colorimetric assay [42]. Briefly, 100 μL of the reaction buffer containing 10 mM KCl, 2 mM ATP, 10 mM $MgCl_2$, 50 mM Tris-HCl (pH 7.5), 150 mM NaCl, and 10 μM proteins, in the absence or the presence of 20 μM GroES were incubated for 1 hour at 37 ˚C. Enzymatic reactions were terminated by addition of 500 μL of 1% SDS. Colour development was measured as follows: 200 μL of

ammonium molybdate reagent was added to each tube immediately followed by the addition of 200 μl Elon reagent. After 15 min at room temperature, the absorbance of the final solution (200 μL of reactions in 96 well-plates) was measured at 700 nm. Control experiments without protein were always included. The recombinant *E. coli* GroEL was from Abcam.

To investigate the effect of metal ions on ATPase activity, the same experiment was performed in the presence of 100 μM of metal ions (Ni^{2+}, Cu^{2+}, Cd^{2+}, Zn^{2+} or Co^{2+}).

Structural modelling of GroEL1

A BLAST search performed on the Protein Data Bank (PDB) sequences identified GroEL2 from *M. tuberculosis* as a potential template for building a GroEL1 model. Two 3D models of GroEL1 were built by comparative modelling with Modeller 9v11 [43] using the *M. tuberculosis* Cpn60.2 (GroEL2) crystal structure as a template [44] and the sequence alignment carried out with ClustalW. The ATP analogue was positioned based on the superposed GroEL structure (PDB ID: 1SX3) [45] to predict the potential ATP binding site.

Results

GroEL1 increases copper tolerance during *M. bovis* BCG biofilm formation

The impact of metal ions was evaluated on the biofilm growth of *M. bovis* BCG strains. As the Δ*groEL1* BCG (KO) strain is more sensitive to glycerol osmotic stress [11], the amount of glycerol in the biofilm culture was reduced to 3.5% (instead of 6%) in order to allow biofilm production by the Δ*groEL1* strain. The wild type (wt) BCG strain was able to form mature biofilm (with ridges and troughs) in the presence of Cu^{2+} concentrations up to 175 μM (**Figure 1**). In contrast, the biofilms of the Δ*groEL*1 strain were already impaired with 100-125 μM Cu^{2+}, showing that loss of GroEL1 enhances mycobacterial susceptibility to copper. Complementation of the *groEL*1 gene in the KO strain fully restored biofilm growth in the presence of Cu^{2+} concentrations up to 175 μM, demonstrating that the loss of GroEL1 is indeed responsible for the enhanced copper susceptibility during biofilm growth (**Figure 1**). This protective effect of GroEL1 was only observed in biofilm culture (Sauton's medium) and not in the planktonic culture (7H9 medium). This could be due to a reduced concentration of free Cu^{2+} concentration in the 7H9 culture, as this medium contains 500 mg/L albumin, well-known to bind Cu^{2+} [46]. Indeed, the minimum inhibitory concentration (MIC) for $CuCl_2$ was identical (150-175 μM) for the three strains in the 7H9 medium.

Does the mutant strain exhibit susceptibility to other metallic ions? To verify this point, biofilm growth was also evaluated in the presence of increasing concentrations of Zn^{2+} and Cd^{2+}. As shown in **Figure S1**, no significant difference in terms of susceptibility to these ions during biofilm growth was observed among the three *M. bovis* BCG strains. Indeed, biofilm cultures were unaffected by Zn^{2+} at concentrations up to 600 μM, which already exceeds the Zn^{2+} concentration inside the infected macrophages [31]. The biofilms of the three

strains were similarly affected in Cd^{2+} concentrations > 5 μM. Thus, the GroEL1 protein does not seem to protect the bacilli from excessive Cd^{2+}. The GroEL1 effect is thus copper specific.

The native histidine-rich region affects GroEL1 stability

To study the role of the C-terminal histidine-rich region (HDHHHGHAH) of GroEL1, the recombinant *M. bovis* BCG proteins GroEL1 and a *M. bovis* GroEL1 devoid of the C-terminal histidine-rich region (GroEL1ΔHis) were purified. These proteins were overproduced in the *E. coli* BL21(DE3) strain, purified by immobilized metal affinity chromatography, treated with human rhinovirus 3C protease for the additional 5×His-tag cleavage, and then further purified by size exclusion chromatography (SEC). The purity and the integrity of recombinant proteins were analysed by SDS-PAGE and mass spectrometry, respectively (**Figure S2**). Mass spectrometry data clearly indicated that the additional N-terminal 5×His-tag was removed in both proteins.

Recombinant GroEL1 was eluted in SEC as a single peak but migrated as two bands in SDS-PAGE analysis, i.e. an upper stronger band followed by a weaker band **(Figure S2 A)**. Peptide sequence analysis by mass spectrometry demonstrated that the weak band corresponds to a degradation product of GroEL1 lacking the N-terminal region (about 45 amino acid residues missing out of 543) (data not shown). This proteolysis was not observed for the GroEL1ΔHis, always showing a single band in SDS-PAGE analysis **(Figure S2 B)**.

GroEL1-copper interaction analysed by native mass spectrometry

To further investigate the interaction between GroEL1 and Cu^{2+}, the metal binding specificity of *M. tuberculosis* GroEL proteins was monitored by native mass spectrometry (**Figure 2**). Native mass spectra were recorded after incubation of the proteins with or without Cu^{2+}. Importantly, the addition of one molar equivalent of Cu^{2+} induced a shift of the GroEL1 peak to a higher m/z

value corresponding to the binding of one atom of copper to the protein (**Figure 2B**). The nearly complete disappearance of the apo peak upon copper addition reflects an effective binding of this metal ion to GroEL1. In contrast, practically no conversion of the apo to the holo form was observed upon addition of one molar equivalent of Cu^{2+} to GroEL1ΔHis (**Figure 2C**). This observation suggests that the Cu^{2+} is mainly bound to the histidine-rich region of GroEL1.

Moreover, the ability of other metal ions (*i.e.* Zn^{2+}, Ni^{2+}, Cd^{2+} and Co^{2+}) to bind to GroEL1 was also assessed (**Figure S3 and S4**). The binding of Zn^{2+} and Ni^{2+} to GroEL1 was also observed but with a lower efficiency than for Cu^{2+} (**Figure S3**). At a metal/protein ratio of 1:1, there were nearly no binding of Cd^{2+} to GroEL1 (**Figure S4**). To further study the copper binding to the protein, GroEL1 was titrated with increasing amounts of Cu^{2+} and analysed by native mass spectrometry (**Figure 3**). Sequential addition of Cu^{2+} led to the appearance of the holo form GroEL1·Cu which was the main population observed at the GroEL1/Cu^{2+} 1:1 molar ratio, as described in the previous experiment. At higher molar ratios, GroEL1·2Cu and GroEL1·3Cu populations were detected with a concomitant decrease of the GroEL1·Cu abundance. On the contrary, in the same range of Cu^{2+} concentrations, the apo form of GroEL1ΔHis did not totally disappear and the highest stoichiometry for the protein/metal complex observed in the presence of four molar equivalents of copper was GroEL1ΔHis·2Cu. For the sake of comparison, the recombinant GroEL2 was also purified (**Figure S2**) and the binding of copper to GroEL2 was also investigated. The binding of copper to GroEL2 gave similar results as the binding of copper to GroEL1ΔHis (**Figure 3**).

The effect of copper on *M. tuberculosis* GroEL1 protein oligomeric state was also investigated by native mass spectrometry (**Figure S5**). The recombinant GroEL1 is mainly monomeric with small amounts of dimeric protein, in agreement with a previous report [47]. The same observations were

obtained for the GroEL1ΔHis and GroEL2 (data not shown). Moreover, when adding Cu^{2+}, the overall spectra for GroEL1 and GroEL1ΔHis did not change significantly in the range of 0 to 30 μM $CuCl_2$, indicating that higher oligomers could not be observed under these conditions.

The effect of copper on GroEL1 thermal stability

Thermal shift assays were performed to evaluate the effect of Cu^{2+} on protein stability. The use of the SYPRO orange fluorescent dye and a real-time thermocycler to follow thermal denaturation in different conditions enabled the monitoring of GroEL1 and GroEL1ΔHis stability in the presence of Cu^{2+}. In the presence of Cu^{2+} (10 to 50 μM), the Tm values for GroEL1 were higher than for GroEL1ΔHis (**Figure 4**). Although high Cu^{2+} concentrations are deleterious for both proteins, the difference in Tm values suggests that the binding of copper to the histidine-rich region could have a protective effect as the binding of the metal ions is more efficient on GroEL1 than on GroEL1ΔHis.

Protease susceptibility assay

To further investigate whether Cu^{2+} could increase the GroEL1 protein stability, a mild trypsin digestion was performed in the absence or the presence of Cu^{2+}. The GroEL1 displayed a higher tolerance to trypsin digestion in the presence of Cu^{2+} (**Figure 5**). In addition, the degree of tolerance increased with the copper concentration (**Figure S6**). The binding of Cu^{2+} to the GroEL1 protein improved thus its stability. A similar result was also observed with GroEL1ΔHis (**Figure 5**). A control was performed using *Nα*-benzoyl-DL-arginine 4-nitroanilide hydrochloride (BAPNA) as substrate and demonstrated that the trypsin activity was not affected by the presence of Cu^{2+} and that the protease even displayed a small increase of activity in the range of copper concentrations used in the experiment (data not shown), as previously reported [48]. The fact that the trypsin susceptibility was also decreased for GroEL1ΔHis in the presence of Cu^{2+}, suggests that conformational changes could also occur

in the protein upon Cu^{2+} binding to the other coordination sites.

Copper increases the GroEL1 ATPase activity

ATP hydrolysis by the recombinant *M. tuberculosis* GroEL proteins was investigated in the presence or absence of metal ions. *M. tuberculosis* GroEL1 and GroEL2 displayed weak ATPase activity, with a higher activity for GroEL2 than for GroEL1 (**Figure 6**). Surprisingly, the GroEL1ΔHis showed a two-fold increased ATPase activity compared to GroEL1. GroEL1ΔHis and GroEL2 had almost the same activity (**Figure 6**). The presence of GroES, also produced and purified for this study (**Figure S2**), had no impact on GroEL1 and GroEL2 *in vitro* ATPase activities, in agreement with previous studies [47, 49]. The GroEL1 ATPase activity was increased about eight-fold in the presence of Cu^{2+} (**Figure 7**). This effect was not observed for GroEL1ΔHis and GroEL2. The other metal ions tested (Ni^{2+}, Co^{2+}, Cd^{2+} or Zn^{2+}) did not influence the GroEL1 protein activity, although the presence of Co^{2+} slightly increased the GroEL1ΔHis and the GroEL2 ATPase activities. The effect of Cu^{2+} and Co^{2+} on recombinant *E. coli* GroEL ATPase activity was also evaluated and showed that these metal ions had no effect on its ATPase activity (**Figure S7**).

GroEL1 three-dimensional model

To better understand the impact of the histidine-rich C-terminal region on the N-terminal region stability, a GroEL1 three-dimensional structure model was built using the crystal structure of *M. tuberculosis* GroEL2 (PDB ID: 3RTK) [44] as template. Both proteins share 62% sequence identity (86% sequence similarity) in 527 residues overlap. It is worth noting that in the crystal structure of GroEL2, the conformation of the 60 first N-terminal residues and of the 26 last C-terminal residues was not solved, most probably due to the flexibility of these domains. The C-terminal residues are also absent in the published structures of the *E. coli* GroEL (*e.g.* PDB ID: 1GRL, 1OEL) [50, 51]. The model of GroEL1 in the present study suggests that the N- and C-terminal domains of the protein could

404 be close to each other in the equatorial domain of the protein (**Figure 8**).

405

Discussion

The GroEL1 protein plays important roles in mycobacterial adaptation to the environment, such as resistance to antibiotic and other various stressful conditions [11, 22, 52]. Copper is on one hand a critical cofactor for various mycobacterial enzymes, including those helping to resist oxidative stress, *i.e.* electron transfer reactions, cytochrome *c* oxidase and Cu/Cu superoxide dismutase, but on the other, high copper concentrations are bactericidal [53, 54].

Our results indicate that high concentrations of Cu^{2+} can reduce *M. bovis* BCG biofilm maturation and that GroEL1 is required to resist to toxic Cu^{2+} concentration under this stress condition. As GroEL1 was unable to protect bacteria against toxic Cd^{2+} concentration, its effect is copper specific. Native mass spectrometry analyses demonstrated the specific binding of copper ions to GroEL1, with a higher affinity for the histidine-rich C-terminal domain. Up to two other binding sites with a lower affinity are most probably present in the protein as deduced from the comparison of the copper binding profiles of GroEL1 and GroEL1ΔHis. The presence of binding sites with different affinities for copper ions was also observed for GroEL1 by isothermal titration calorimetry (ITC) analysis [34].

Ansari *et al*. observed similar results using *M. tuberculosis* strains, however in normal growth condition [34]. They didn't investigate the role of GroEL1 under stress conditions [34]. The fact that they observed an involvement of GroEL1 to mitigate Cu^{2+} toxicity in planktonic growth conditions, which was not detected by our group, could be due either to the use of a different mycobacterium species or to our optimal planktonic growth conditions for *M. bovis* BCG (*i.e.* optimized albumin quality), leading to less GroEL1 production or increased Cu^{2+} capture by our albumin in the 7H9 planktonic cultures [46].

The presence of the Cu^{2+} binding sites on GroEL1 but also the protective role of GroEL1 against high toxic copper concentrations, strongly suggests that this protein could segregate *in vivo* the copper ions present in the macrophage phagosomes [32] and therefore, by decreasing the concentration of free ions, protect bacteria from the bactericidal toxic effect of this metal ion. Usually, copper resistance mechanisms involve copper specific chaperones, storage proteins and efflux systems [55]. In *M. tuberculosis*, various P-type ATPases,

generally induced in stressful conditions, have been reported as possible transporters of heavy-metal cations [56]. For instance, CtpV and CtpC are induced by the intraphagosomal concentrations of Cu^{+} and Zn^{2+} [57, 58]. Interestingly, although the *E. coli cop*A gene (ortholog of *ctp*V) encodes two proteins with identical N-terminus, a copper chaperone and a copper transporter [59], neither literature search, nor CtpV/CopA aa Clustal sequence alignment allowed to identify a similar copper chaperone for *M. tuberculosis*. In addition, mycobacterial maintenance of low intracellular Cu concentrations also necessitates MctB, a putative copper transport protein at the outer membrane [60]. The metallothionein MymT, a cysteine-rich protein, able to bind up to six Cu^{+}, partially involved in copper toxicity resistance, could play the role of a storage protein [61]. Furthermore, a copper inducible *M. tuberculosis* operon, including *lpqS* (encoding a putative lipoprotein), *mmcO* (encoding a mycobacterial multicopper oxidase), *Rv2963* (encoding a possible permease), *mymT* (encoding the metallothionein described above), *socAB* (small ORF induced by Cu A and B) and *ricR* (encoding a repressor of this operon) genes, seems to provide key components of an additional system involved in copper detoxification [30]. All these previously reported mechanisms could help the bacilli to maintain the copper homeostasis in *M. tuberculosis* [30, 62]. However, they seem to lack a key component: a copper chaperone which could shuttle copper to the above mentioned copper binding proteins and efflux pumps [30]. We hypothesized that GroEL1 could possibly function as such a copper-shuttling chaperone, as GroEL1 can be secreted in the culture filtrate [22].

As the recombinant GroEL1ΔHis is less prone to the N-terminal proteolytic degradation during purification (**Figure S2**), we hypothesize that the histidine-rich region in GroEL1 somehow increases the accessibility of the latter to proteolytic enzymes. Although this C-terminal histidine-rich region is involved in GroEL1 destabilisation, the stability of this protein seems improved in the presence of Cu^{2+} binding. Apart from this protective role against higher bactericidal copper concentration, the binding of copper ions to GroEL1 could also have an additional function to improve the GroEL1 N-terminal region stability.

Brazil *et al*. reported that the divalent cations (Ca^{2+}, Mg^{2+}, Mn^{2+}, Zn^{2+}) induce exposure of the *E. coli* GroEL hydrophobic surfaces and strengthen the GroEL hydrophobic binding interactions [63]. This was attributed to a conformation change of GroEL when binding to the divalent cations [64]. Based on our GroEL1 3D model, it is possible that the N- and C-terminal domains of the protein could be close to each other and that the binding of copper ions to the histidine-rich domain could affect the interaction of C-terminal segment with the N-terminal domain thereby reducing the exposure of the latter to proteases. Nevertheless, copper binding is not inducing a modification of the GroEL1 oligomeric state, as demonstrated by native mass spectrometry analysis.

Interestingly, Ansari *et al*., also built a GroEL1 3D model based on their small angle X-ray scattering (SAXS) data obtained in the presence of various GroEL1/Cu^{2+} ratios [34]. The SAXS analysis suggested that the protein adopts a more open structure in the presence of Cu^{2+} and becomes more flexible. These conformational changes could be responsible for the increase of GroEL1 ATPase activity observed in our study in the presence of copper ions. As the protein is predicted to be more extended and flexible in the presence of Cu^{2+}, it would be expected that GroEL1 would be more susceptible to protease activity. However, this is not what was observed as our limited trypsin digestion assay suggested that GroEL1, especially the N-terminal region, is less accessible to the protease in the presence of Cu^{2+}.

Importantly, the GroEL1 ATPase activity is drastically and specifically increased in the presence of Cu^{2+}, mainly binding to the histidine-rich region. This is only observed for GroEL1 and not for GroEL1ΔHis, GroEL2 and *E. coli* GroEL, suggesting that the binding of copper ions to the GroEL1 histidine-rich C-terminal region induces a conformational change allowing to increase its ATPase activity. This could be due to the GroEL1 stability improvement in the presence of Cu^{2+}. Therefore, in the absence of Cu^{2+}, GroEL1ΔHis and GroEL2, both lacking the histidine-rich region, displayed higher ATPase activity than the GroEL1 possibly because of their higher protein stability. However, in the presence of Cu^{2+}, GroEL1 and GroEL2 show similar ATPase activity.

Conclusions

Here, we propose a novel role for the *M. tuberculosis* GroEL1. This protein could be involved in copper resistance during mycobacterial biofilm formation potentially by acting as a metal storage protein. Therefore, when mycobacteria encounter high copper concentrations, as in the macrophage, GroEL1, by binding copper, could help bacteria to tolerate high copper concentrations and consequently this bactericidal stress.

Conflicts of interest

The authors declare that they have no conflicts of interest with the content of this article.

Acknowledgment

This work was partially supported by the China Scholarship Council (CSC) (No.201408210159). F.S. and D.P.K. would like to thank James Ault and Rachel George for their help operating the Orbitrap UHMR. The Orbitrap UHMR was funded by Wellcome Trust multi-user equipment grant 208385/Z/17/Z.

References

1. WHO, Global tuberculosis report, *World Health Organization*, 2019.
2. P. J. Brennan and H. Nikaido, The envelope of mycobacteria, *Annu Rev Biochem*, 1995, **64**, 29-63.
3. M. Jankute, J. A. Cox, J. Harrison and G. S. Besra, Assembly of the Mycobacterial Cell Wall, *Annu Rev Microbiol*, 2015, **69**, 405-423.
4. L. R. Camacho, P. Constant, C. Raynaud, M. A. Laneelle, J. A. Triccas, B. Gicquel, M. Daffe and C. Guilhot, Analysis of the phthiocerol dimycocerosate locus of *Mycobacterium tuberculosis*. Evidence that this lipid is involved in the cell wall permeability barrier, *The Journal of biological chemistry*, 2001, **276**, 19845-19854.
5. K. Soetaert, C. Rens, X. M. Wang, J. De Bruyn, M. A. Laneelle, F. Laval, A. Lemassu, M. Daffe, P. Bifani, V. Fontaine and P. Lefevre, Increased Vancomycin Susceptibility in Mycobacteria: a New Approach To Identify Synergistic Activity against Multidrug-Resistant Mycobacteria, *Antimicrobial agents and chemotherapy*, 2015, **59**, 5057-5060.
6. C. W. Hall and T. F. Mah, Molecular mechanisms of biofilm-based antibiotic resistance and tolerance in pathogenic bacteria, *FEMS Microbiol Rev*, 2017, **41**, 276-301.
7. A. Queiroz and L. W. Riley, Bacterial immunostat: *Mycobacterium tuberculosis* lipids and their role in the host immune response, *Rev Soc Bras Med Trop*, 2017, **50**, 9-18.
8. V. Sundaramurthy, H. Korf, A. Singla, N. Scherr, L. Nguyen, G. Ferrari, R. Landmann, K. Huygen and J. Pieters, Survival of *Mycobacterium tuberculosis* and *Mycobacterium bovis* BCG in lysosomes *in vivo*, *Microbes Infect*, 2017, **19**, 515-526.
9. A. M. Alnimr, Dormancy models for *Mycobacterium tuberculosis*: A minireview, *Braz J Microbiol*, 2015, **46**, 641-647.

548 10. R. D. Turner, C. Chiu, G. J. Churchyard, H. Esmail, D. M. Lewinsohn, N. R.
549 Gandhi and K. P. Fennelly, Tuberculosis Infectiousness and Host Susceptibility,
550 *J Infect Dis*, 2017, **216**, S636-S643.
551 11. S. Zeng, P. Constant, D. Yang, A. Baulard, P. Lefevre, M. Daffe, R. Wattiez
552 and V. Fontaine, Cpn60.1 (GroEL1) Contributes to Mycobacterial Crabtree
553 Effect: Implications for Biofilm Formation, *Front Microbiol*, 2019, **10**, 1149.
554 12. T. H. Kong, A. R. Coates, P. D. Butcher, C. J. Hickman and T. M. Shinnick,
555 *Mycobacterium tuberculosis* expresses two chaperonin-60 homologs,
556 *Proceedings of the National Academy of Sciences of the United States of*
557 *America*, 1993, **90**, 2608-2612.
558 13. A. Ojha, M. Anand, A. Bhatt, L. Kremer, W. R. Jacobs and G. F. Hatfull,
559 GroEL1: A Dedicated Chaperone Involved in Mycolic Acid Biosynthesis during
560 Biofilm Formation in Mycobacteria, *Cell*, 2005, **123**, 861-873.
561 14. C. Chaudhry, G. W. Farr, M. J. Todd, H. S. Rye, A. T. Brunger, P. D. Adams,
562 A. L. Horwich and P. B. Sigler, Role of the gamma-phosphate of ATP in
563 triggering protein folding by GroEL-GroES: function, structure and energetics,
564 *EMBO J*, 2003, **22**, 4877-4887.
565 15. H. S. Rye, A. M. Roseman, S. Chen, K. Furtak, W. A. Fenton, H. R. Saibil
566 and A. L. Horwich, GroEL-GroES cycling: ATP and nonnative polypeptide direct
567 alternation of folding-active rings, *Cell*, 1999, **97**, 325-338.
568 16. T. E. Gray and A. R. Fersht, Cooperativity in ATP hydrolysis by GroEL is
569 increased by GroES, *FEBS Lett*, 1991, **292**, 254-258.
570 17. M. J. Todd, P. V. Viitanen and G. H. Lorimer, Hydrolysis of adenosine 5'-
571 triphosphate by *Escherichia coli* GroEL: effects of GroES and potassium ion,
572 *Biochemistry*, 1993, **32**, 8560-8567.
573 18. P. V. Viitanen, T. H. Lubben, J. Reed, P. Goloubinoff, D. P. O'Keefe and G.
574 H. Lorimer, Chaperonin-facilitated refolding of ribulose bisphosphate
575 carboxylase and ATP hydrolysis by chaperonin 60 (groEL) are K^+ dependent,

576 *Biochemistry*, 1990, **29**, 5665-5671.
577 19. G. C. Melkani, G. Zardeneta and J. A. Mendoza, The ATPase activity of
578 GroEL is supported at high temperatures by divalent cations that stabilize its
579 structure, *Biometals : an international journal on the role of metal ions in biology,*
580 *biochemistry, and medicine*, 2003, **16**, 479-484.
581 20. G. R. Stewart, L. Wernisch, R. Stabler, J. A. Mangan, J. Hinds, K. G. Laing,
582 D. B. Young and P. D. Butcher, Dissection of the heat-shock response in
583 *Mycobacterium tuberculosis* using mutants and microarrays, *Microbiology*,
584 2002, **148**, 3129-3138.
585 21. N. S. Dosanjh, M. Rawat, J. H. Chung and Y. Av-Gay, Thiol specific
586 oxidative stress response in Mycobacteria, *FEMS Microbiol Lett*, 2005, **249**, 87-
587 94.
588 22. X. M. Wang, C. Lu, K. Soetaert, C. S'Heeren, P. Peirs, M. A. Laneelle, P.
589 Lefevre, P. Bifani, J. Content, M. Daffe, K. Huygen, J. De Bruyn and R. Wattiez,
590 Biochemical and immunological characterization of a *cpn60.1* knockout mutant
591 of *Mycobacterium bovis* BCG, *Microbiology*, 2011, **157**, 1205-1219.
592 23. Y. Hu, B. Henderson, P. A. Lund, P. Tormay, M. T. Ahmed, S. S. Gurcha,
593 G. S. Besra and A. R. Coates, A *Mycobacterium tuberculosis* mutant lacking
594 the *groEL* homologue *cpn60.1* is viable but fails to induce an inflammatory
595 response in animal models of infection, *Infect Immun*, 2008, **76**, 1535-1546.
596 24. I. M. Monahan, J. Betts, D. K. Banerjee and P. D. Butcher, Differential
597 expression of mycobacterial proteins following phagocytosis by macrophages,
598 *Microbiology*, 2001, **147**, 459-471.
599 25. J. Esteban and M. Garcia-Coca, Mycobacterium Biofilms, *Front Microbiol*,
600 2017, **8**, 2651.
601 26. G. Carter, M. Wu, D. C. Drummond and L. E. Bermudez, Characterization
602 of biofilm formation by clinical isolates of *Mycobacterium avium*, *J Med*
603 *Microbiol*, 2003, **52**, 747-752.

27. A. K. Ojha, A. D. Baughn, D. Sambandan, T. Hsu, X. Trivelli, Y. Guerardel, A. Alahari, L. Kremer, W. R. Jacobs, Jr. and G. F. Hatfull, Growth of *Mycobacterium tuberculosis* biofilms containing free mycolic acids and harbouring drug-tolerant bacteria, *Molecular microbiology*, 2008, **69**, 164-174.
28. H. Botella, P. Peyron, F. Levillain, R. Poincloux, Y. Poquet, I. Brandli, C. Wang, L. Tailleux, S. Tilleul, G. M. Charriere, S. J. Waddell, M. Foti, G. Lugo-Villarino, Q. Gao, I. Maridonneau-Parini, P. D. Butcher, P. R. Castagnoli, B. Gicquel, C. de Chastellier and O. Neyrolles, Mycobacterial p(1)-type ATPases mediate resistance to zinc poisoning in human macrophages, *Cell Host Microbe*, 2011, **10**, 248-259.
29. V. Hodgkinson and M. J. Petris, Copper homeostasis at the host-pathogen interface, *The Journal of biological chemistry*, 2012, **287**, 13549-13555.
30. X. Shi and K. H. Darwin, Copper homeostasis in *Mycobacterium tuberculosis*, *Metallomics : integrated biometal science*, 2015, **7**, 929-934.
31. D. Wagner, J. Maser, B. Lai, Z. Cai, C. E. Barry, K. Honer zu Bentrup, D. G. Russell and L. E. Bermudez, Elemental Analysis of *Mycobacterium avium*-, *Mycobacterium tuberculosis*-, and *Mycobacterium smegmatis*-Containing Phagosomes Indicates Pathogen-Induced Microenvironments within the Host Cell's Endosomal System, *The Journal of Immunology*, 2005, **174**, 1491-1500.
32. F. Wolschendorf, D. Ackart, T. B. Shrestha, L. Hascall-Dove, S. Nolan, G. Lamichhane, Y. Wang, S. H. Bossmann, R. J. Basaraba and M. Niederweis, Copper resistance is essential for virulence of *Mycobacterium tuberculosis*, *Proceedings of the National Academy of Sciences of the United States of America*, 2011, **108**, 1621-1626.
33. O. Neyrolles, F. Wolschendorf, A. Mitra and M. Niederweis, Mycobacteria, metals, and the macrophage, *Immunological reviews*, 2015, **264**, 249-263.
34. M. Y. Ansari, S. D. Batra, H. Ojha, Ashish, J. S. Tyagi and S. C. Mande, A novel function of *M. tuberculosis* chaperonin paralog GroEL1 in copper

632 homeostasis, *bioRxiv*, 2019, DOI: 10.1101/766162, 766162.
633 35. D. Yang, G. Vandenbussche, D. Vertommen, D. Evrard, R. Abskharon, J.
634 F. Cavalier, G. Berger, S. Canaan, M. S. Khan, S. Zeng, A. Wohlkonig, M.
635 Prevost, P. Soumillion and V. Fontaine, Methyl arachidonyl fluorophosphonate
636 inhibits *Mycobacterium tuberculosis* thioesterase TesA and globally affects
637 vancomycin susceptibility, *FEBS Lett*, 2020, **594**, 79-93.
638 36. C. Structural Genomics, C. China Structural Genomics, C. Northeast
639 Structural Genomics, S. Graslund, P. Nordlund, J. Weigelt, B. M. Hallberg, J.
640 Bray, O. Gileadi, S. Knapp, U. Oppermann, C. Arrowsmith, R. Hui, J. Ming, S.
641 dhe-Paganon, H. W. Park, A. Savchenko, A. Yee, A. Edwards, R. Vincentelli,
642 C. Cambillau, R. Kim, S. H. Kim, Z. Rao, Y. Shi, T. C. Terwilliger, C. Y. Kim, L.
643 W. Hung, G. S. Waldo, Y. Peleg, S. Albeck, T. Unger, O. Dym, J. Prilusky, J. L.
644 Sussman, R. C. Stevens, S. A. Lesley, I. A. Wilson, A. Joachimiak, F. Collart, I.
645 Dementieva, M. I. Donnelly, W. H. Eschenfeldt, Y. Kim, L. Stols, R. Wu, M. Zhou,
646 S. K. Burley, J. S. Emtage, J. M. Sauder, D. Thompson, K. Bain, J. Luz, T.
647 Gheyi, F. Zhang, S. Atwell, S. C. Almo, J. B. Bonanno, A. Fiser, S.
648 Swaminathan, F. W. Studier, M. R. Chance, A. Sali, T. B. Acton, R. Xiao, L.
649 Zhao, L. C. Ma, J. F. Hunt, L. Tong, K. Cunningham, M. Inouye, S. Anderson,
650 H. Janjua, R. Shastry, C. K. Ho, D. Wang, H. Wang, M. Jiang, G. T. Montelione,
651 D. I. Stuart, R. J. Owens, S. Daenke, A. Schutz, U. Heinemann, S. Yokoyama,
652 K. Bussow and K. C. Gunsalus, Protein production and purification, *Nat*
653 *Methods*, 2008, **5**, 135-146.
654 37. M. R. Wilkins, E. Gasteiger, A. Bairoch, J. C. Sanchez, K. L. Williams, R. D.
655 Appel and D. F. Hochstrasser, Protein identification and analysis tools in the
656 ExPASy server, *Methods Mol Biol*, 1999, **112**, 531-552.
657 38. M. T. Marty, A. J. Baldwin, E. G. Marklund, G. K. Hochberg, J. L. Benesch
658 and C. V. Robinson, Bayesian deconvolution of mass and ion mobility spectra:
659 from binary interactions to polydisperse ensembles, *Anal Chem*, 2015, **87**,

660 4370-4376.
661 39. K. Huynh and C. L. Partch, Analysis of protein stability and ligand
662 interactions by thermal shift assay, *Curr Protoc Protein Sci*, 2015, **79**, 28 29 21-
663 28 29 14.
664 40. H. Kawasaki, Y. Kurosu, H. Kasai, T. Isobe and T. Okuyama, Limited
665 digestion of calmodulin with trypsin in the presence or absence of various metal
666 ions, *J Biochem*, 1986, **99**, 1409-1416.
667 41. I. Kurtovic, S. N. Marshall and B. K. Simpson, Isolation and characterization
668 of a trypsin fraction from the pyloric ceca of chinook salmon (*Oncorhynchus*
669 *tshawytscha*), *Comp Biochem Physiol B Biochem Mol Biol*, 2006, **143**, 432-440.
670 42. , Biomembranes. Part Q. ATP-driven pumps and related transport: calcium,
671 proton, and potassium pumps, *Methods Enzymol*, 1988, **157**, 1-731.
672 43. A. Fiser and A. Sali, Modeller: generation and refinement of homology-
673 based protein structure models, *Methods Enzymol*, 2003, **374**, 461-491.
674 44. A. Shahar, M. Melamed-Frank, Y. Kashi, L. Shimon and N. Adir, The
675 dimeric structure of the Cpn60.2 chaperonin of *Mycobacterium tuberculosis* at
676 2.8 Å reveals possible modes of function, *J Mol Biol*, 2011, **412**, 192-203.
677 45. D. K. Clare, P. J. Bakkes, H. van Heerikhuizen, S. M. van der Vies and H.
678 R. Saibil, An expanded protein folding cage in the GroEL-gp31 complex, *J Mol*
679 *Biol*, 2006, **358**, 905-911.
680 46. M. Moriya, Y. H. Ho, A. Grana, L. Nguyen, A. Alvarez, R. Jamil, M. L.
681 Ackland, A. Michalczyk, P. Hamer, D. Ramos, S. Kim, J. F. Mercer and M. C.
682 Linder, Copper is taken up efficiently from albumin and α_2-macroglobulin by
683 cultured human cells by more than one mechanism, *Am J Physiol Cell Physiol*,
684 2008, **295**, C708-721.
685 47. R. Qamra, V. Srinivas and S. C. Mande, *Mycobacterium tuberculosis* GroEL
686 homologues unusually exist as lower oligomers and retain the ability to
687 suppress aggregation of substrate proteins, *J Mol Biol*, 2004, **342**, 605-617.

688 48. H. Steinhart, R. Wieninger-Rustemeyer and M. Kirchgessner, Effect of Cu^{2+}
689 ions on the activity of trypsin on natural substance, *Arch Tierernahr*, 1981, **31**,
690 119-125.
691 49. C. M. Kumar, G. Khare, C. V. Srikanth, A. K. Tyagi, A. A. Sardesai and S.
692 C. Mande, Facilitated oligomerization of mycobacterial GroEL: evidence for
693 phosphorylation-mediated oligomerization, *J Bacteriol*, 2009, **191**, 6525-6538.
694 50. K. Braig, Z. Otwinowski, R. Hegde, D. C. Boisvert, A. Joachimiak, A. L.
695 Horwich and P. B. Sigler, The crystal structure of the bacterial chaperonin
696 GroEL at 2.8 Å, *Nature*, 1994, **371**, 578-586.
697 51. K. Braig, P. D. Adams and A. T. Brunger, Conformational variability in the
698 refined structure of the chaperonin GroEL at 2.8 Å resolution, *Nat Struct Biol*,
699 1995, **2**, 1083-1094.
700 52. A. Sharma, T. Rustad, G. Mahajan, A. Kumar, K. V. Rao, S. Banerjee, D.
701 R. Sherman and S. C. Mande, Towards understanding the biological function
702 of the unusual chaperonin Cpn60.1 (GroEL1) of *Mycobacterium tuberculosis*,
703 *Tuberculosis (Edinb)*, 2016, **97**, 137-146.
704 53. L. Spagnolo, I. Toro, M. D'Orazio, P. O'Neill, J. Z. Pedersen, O. Carugo, G.
705 Rotilio, A. Battistoni and K. Djinovic-Carugo, Unique features of the *sodC*-
706 encoded superoxide dismutase from *Mycobacterium tuberculosis*, a fully
707 functional copper-containing enzyme lacking zinc in the active site, *The Journal*
708 *of biological chemistry*, 2004, **279**, 33447-33455.
709 54. S. K. Ward, B. Abomoelak, E. A. Hoye, H. Steinberg and A. M. Talaat, CtpV:
710 a putative copper exporter required for full virulence of *Mycobacterium*
711 *tuberculosis*, *Molecular microbiology*, 2010, **77**, 1096-1110.
712 55. T. D. Rae, P. J. Schmidt, R. A. Pufahl, V. C. Culotta and T. V. O'Halloran,
713 Undetectable intracellular free copper: the requirement of a copper chaperone
714 for superoxide dismutase, *Science*, 1999, **284**, 805-808.
715 56. L. Novoa-Aponte, A. Leon-Torres, M. Patino-Ruiz, J. Cuesta-Bernal, L. M.

716 Salazar, D. Landsman, L. Marino-Ramirez and C. Y. Soto, In silico identification
717 and characterization of the ion transport specificity for P-type ATPases in the
718 *Mycobacterium tuberculosis* complex, *BMC Struct Biol*, 2012, **12**, 25.
719 57. M. A. Forrellad, L. I. Klepp, A. Gioffre, J. Sabio y Garcia, H. R. Morbidoni,
720 M. de la Paz Santangelo, A. A. Cataldi and F. Bigi, Virulence factors of the
721 *Mycobacterium tuberculosis* complex, *Virulence*, 2013, **4**, 3-66.
722 58. S. K. Ward, E. A. Hoye and A. M. Talaat, The global responses of
723 *Mycobacterium tuberculosis* to physiological levels of copper, *J Bacteriol*, 2008,
724 **190**, 2939-2946.
725 59. S. Meydan, D. Klepacki, S. Karthikeyan, T. Margus, P. Thomas, J. E. Jones,
726 Y. Khan, J. Briggs, J. D. Dinman, N. Vazquez-Laslop and A. S. Mankin,
727 Programmed Ribosomal Frameshifting Generates a Copper Transporter and a
728 Copper Chaperone from the Same Gene, *Mol Cell*, 2017, **65**, 207-219.
729 60. A. Senju and G. Csibra, Gaze following in human infants depends on
730 communicative signals, *Curr Biol*, 2008, **18**, 668-671.
731 61. B. Gold, H. Deng, R. Bryk, D. Vargas, D. Eliezer, J. Roberts, X. Jiang and
732 C. Nathan, Identification of a copper-binding metallothionein in pathogenic
733 mycobacteria, *Nat Chem Biol*, 2008, **4**, 609-616.
734 62. M. I. Samanovic, C. Ding, D. J. Thiele and K. H. Darwin, Copper in microbial
735 pathogenesis: meddling with the metal, *Cell Host Microbe*, 2012, **11**, 106-115.
736 63. B. T. Brazil, J. Ybarra and P. M. Horowitz, Divalent cations can induce the
737 exposure of GroEL hydrophobic surfaces and strengthen GroEL hydrophobic
738 binding interactions. Novel effects of Zn^{2+} GroEL interactions, *The Journal of*
739 *biological chemistry*, 1998, **273**, 3257-3263.
740 64. D. L. Gibbons and P. M. Horowitz, Ligand-induced conformational changes
741 in the apical domain of the chaperonin GroEL, *The Journal of biological*
742 *chemistry*, 1996, **271**, 238-243.
743

Supplementary information

Figure S1. The impact of Zn^{2+} and Cd^{2+} on the various *M. bovis* BCG strains biofilm formation.

Figure S2. Recombinant protein purity and integrity determination.

Figure S3. Native nano-ESI mass spectra of GroEL1 in the absence or presence of Zn^{2+}, Ni^{2+} or Co^{2+}.

Figure S4. Native nano-ESI mass spectra of GroEL1 in the absence or presence of Cd^{2+}.

Figure S5. GroEL1 oligomeric state determination by native mass spectrometry.

Figure S6. Protection of GroEL1 from limited trypsin digestion in a Cu^{2+} concentration dependent manner.

Figure S7. *E. coli* GroEL ATPase activity in the presence of Cu^{2+} and Co^{2+}.

Table S1. Plasmids and oligonucleotide primers.

Figure Legends

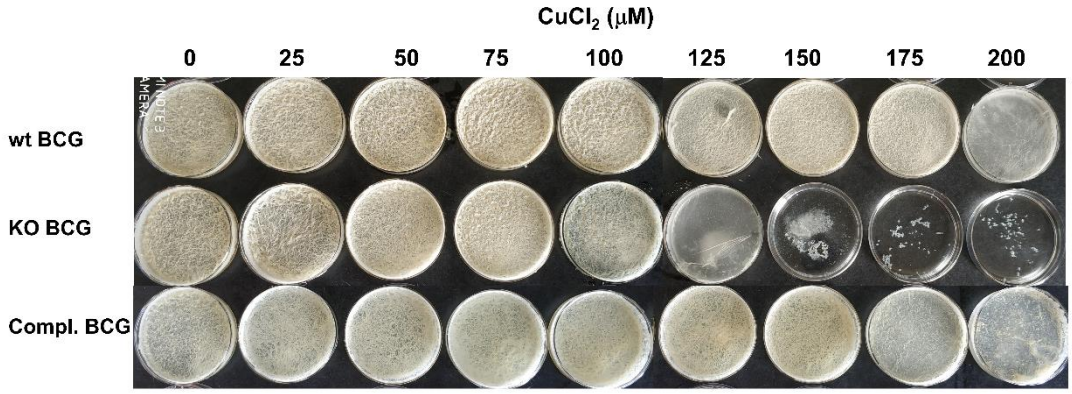

Figure 1. Impact of Cu^{2+} on biofilm formation of various *M. bovis* BCG strains. Biofilm cultures of wild type (wt), Δ*groEL1* (KO), KO complemented (compl.) *M. bovis* BCG strains were grown in 3.5 % glycerol Sauton's medium in the absence or presence of various concentration of $CuCl_2$ for three weeks. Photos shown are representative of at least three different experiments.

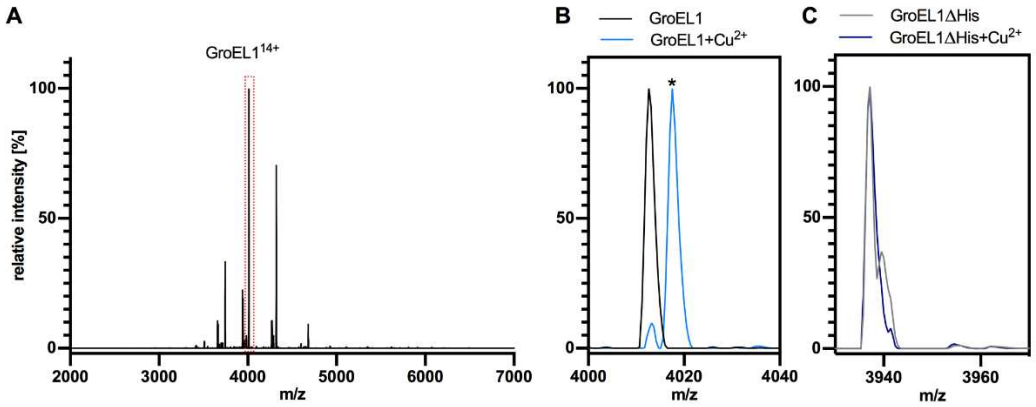

Figure 2. Native nano-ESI spectra of the GroEL1 and the GroEL1ΔHis variant showing different affinities for Cu^{2+}. The protein concentration was 7.5 µM in 500 mM ammonium acetate. (A) Full native mass spectrum of apo GroEL1 shows a narrow charge state distribution with the main charge state $[M + 14H]^{14+}$ highlighted in red. (B) Cu^{2+} binding to GroEL1 shown for the $GroEL1^{14+}$ charge state. A peak shift can be observed upon addition of an equimolar amount of Cu^{2+}, the peak for copper-bound GroEL1 is highlighted with an asterisk. (C) $GroEL1\Delta His^{14+}$ in the presence and absence of one molar equivalent of Cu^{2+}, showing no binding.

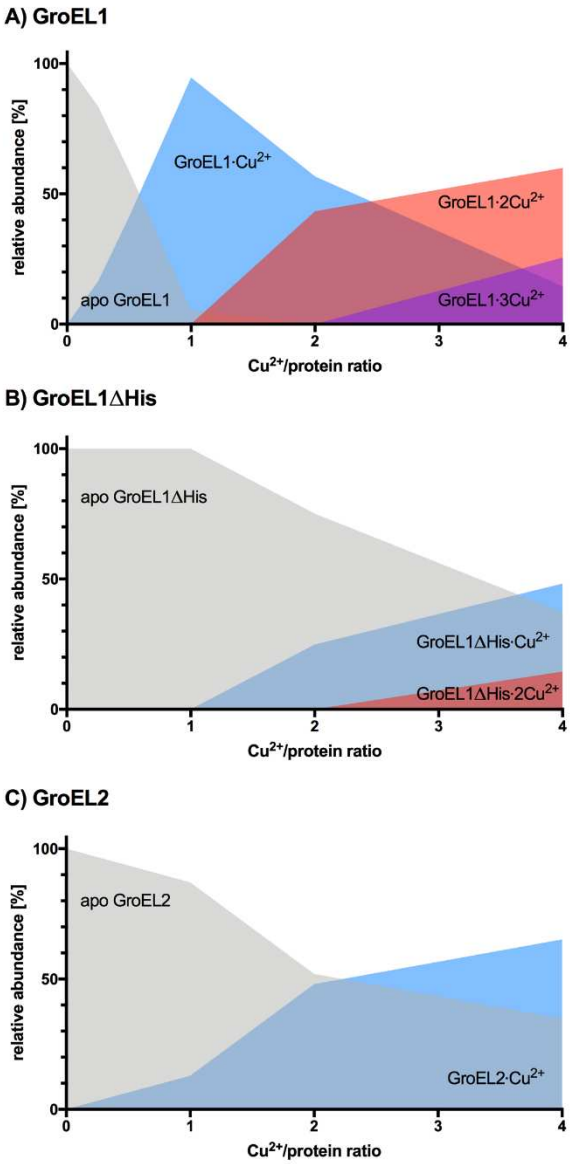

Figure 3. Relative abundance of the different protein-Cu adducts as determined by native mass spectrometry. (A) GroEL1; (B) GroEL1ΔHis; (C) GroEL2. The spectra were recorded at a final protein concentration of 7.5 μM in 500 mM ammonium acetate. Grey, blue, red and purple areas indicate the abundance of apo-protein, 1:1 complex, 2:1 complex and 3:1 complex of protein and Cu^{2+}, respectively. The titration with $CuCl_2$ was performed at molar ratios Cu^{2+} to protein of 0.25:1, 0.5:1, 1:1, 2:1, and 4:1, corresponding to 1.9-30 μM $CuCl_2$. Populations with < 5% intensity are not shown.

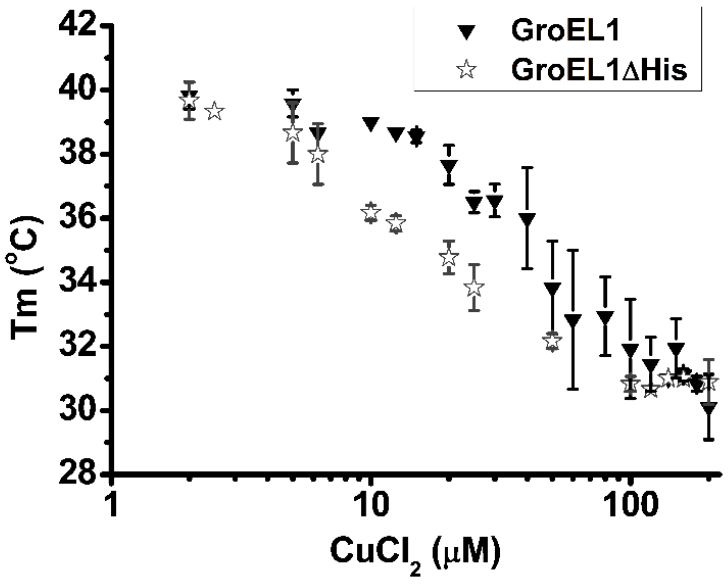

788

789 **Figure 4.** Thermal shift assay to analyse the effect of copper on GroEL1 protein
790 destabilization. The reaction (25 μL) contained 5 μM protein (GroEL1 or
791 GroEL1ΔHis), 0.3 μL of 5000 × SYPRO Orange, with various concentration of
792 $CuCl_2$ in 5 mM HEPES, pH 7.5. The data correspond to mean and standard
793 deviations and were obtained from three independent experiments.

794

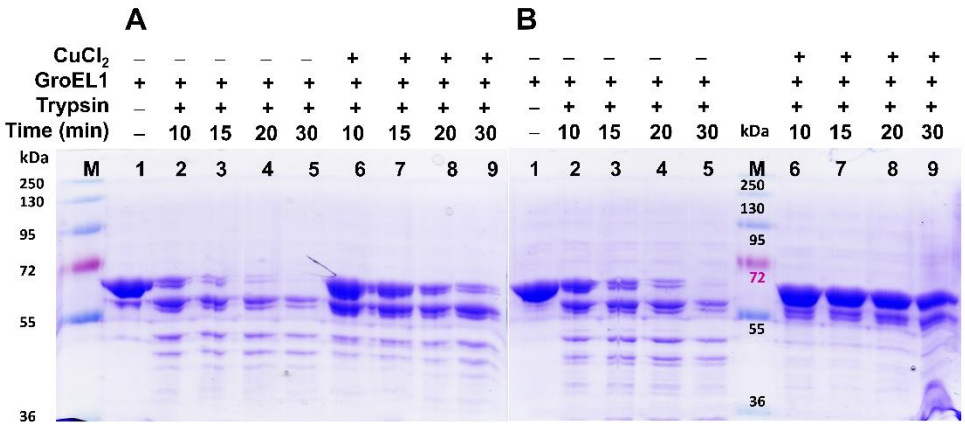

795

796

797 **Figure 5.** Limited trypsin digestion of GroEL1 (A) and GroEL1ΔHis (B) in the
798 absence or the presence of Cu^{2+}. The reaction was stopped at different times
799 (10, 15, 20, 30 min) by adding PMSF. The reaction products were analysed by
800 15% SDS-PAGE. Lane M: molecular mass standards; lane 1-9: 5 μg (~9 μM)
801 of GroEL1 (or GroEL1ΔHis); lane 2 to 5: digestion for 10, 15, 20, 30 min,
802 respectively, in the absence of Cu^{2+}; lane 6 to 9: digestion for 10, 15, 20, 30
803 min, respectively, in the presence of 18 μM Cu^{2+}. The figure is representative
804 of three independent experiments.

805

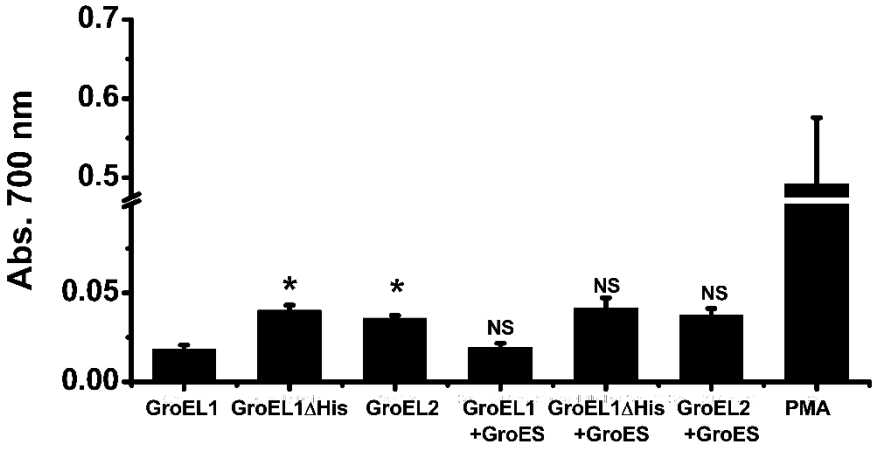

Figure 6. *M. tuberculosis* GroEL protein ATPase activity.

Enzymatic reactions were incubated with 10 μM GroEL and 20 μM GroES proteins at 37 °C for 1 h and the absorbance was recorded at 700 nm. Plasma membrane ATPase (PMA) was used as control. The mean from at least three independent experiments for individual data sets was calculated and plotted along with the standard deviation.

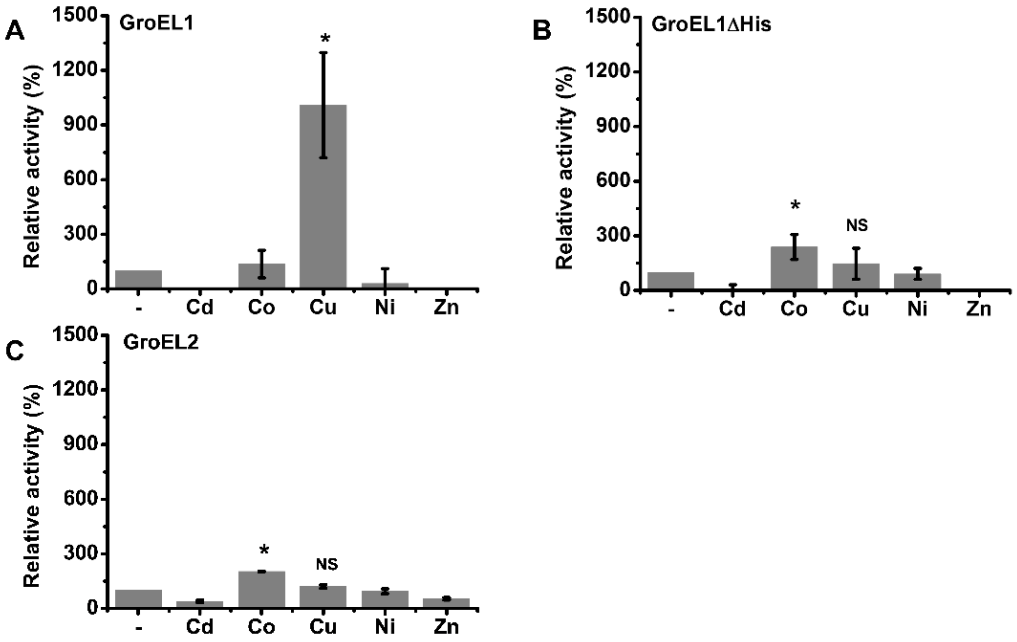

814

815 **Figure 7.** ATPase activity of 10 μM *M. tuberculosis* GroEL proteins in the
816 presence of 100 μM metal ions. (A) GroEL1, (B) GroEL1ΔHis and (C) GroEL2.
817 The mean from at least three independent experiments for individual data sets
818 was calculated and plotted along with the standard deviation, considering the
819 activity measured in the absence of metal ions as 100%.

820

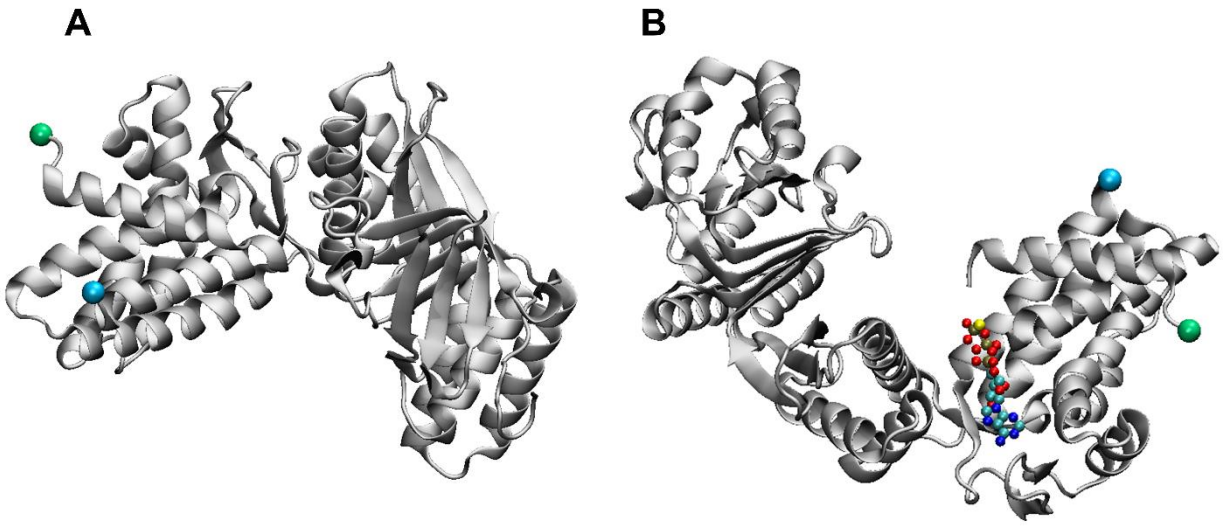

821

822 **Figure 8.** 3D model of GroEL1 represented as a silver cartoon without (A) or
823 with ATP analogue (B). The location of an ATP analog (ATPγS) results from the
824 superposition of the 3D model with the crystal structure of *E. coli* GroEL (PDB
825 ID: 1SX3). The Cα of the first (residue number 61) and last (residue 518) of the
826 model are shown as green and blue van der Waals spheres respectively.
827 [1]